

# AN AERIAL RADIOLOGICAL SURVEY OF THE SUPERCONDUCTING SUPER COLLIDER LABORATORY AND SURROUNDING AREA

WAXAHACHIE, TEXAS

DATE OF SURVEY: JULY-AUGUST 1991

A. E. Fritzsche  
Project Scientist

REVIEWED BY

Harvey W. Clark Jr.

H. W. Clark, Jr., Manager  
Nuclear Radiation Department

This Document is UNCLASSIFIED

C. K. Mitchell

C. K. Mitchell  
Classification Officer

This work was performed by EG&G/EM for the United States Department of Energy under Contract Number DE-AC08-93NV11265.

MASTER

RB

## **ABSTRACT**

An aerial radiological survey was conducted over the Superconducting Super Collider Laboratory (SSCL) site from July 22 through August 20, 1991. Parallel lines were flown at intervals of 305 meters over a 1,036-square-kilometer (400-square-mile) area surrounding Waxahachie, Texas. The 70,000 terrestrial gamma energy spectra obtained were reduced to an exposure rate contour map overlaid on a United States Geological Survey (USGS) map of the area. The mean terrestrial exposure rate measured was 5.4  $\mu\text{R}/\text{h}$  at 1 meter above ground level. Comparison to ground-based measurements shows good agreement. No anomalous or man-made isotopes were detected.

# CONTENTS

|                       |    |
|-----------------------|----|
| <b>Abstract</b> ..... | ii |
|-----------------------|----|

## **Sections**

|  |    |
|--|----|
| <b>1.0</b> <b>Introduction</b> .....                           | 1  |
| <b>2.0</b> <b>Survey Site Description</b> .....                | 1  |
| <b>3.0</b> <b>Survey Equipment and Methods</b> .....           | 1  |
| <b>3.1</b> <b>Aircraft System</b> .....                        | 1  |
| <b>3.2</b> <b>Data Van</b> .....                               | 2  |
| <b>3.3</b> <b>Survey Method</b> .....                          | 2  |
| <b>3.4</b> <b>Ground-Based Measurements</b> .....              | 2  |
| <b>4.0</b> <b>General Data Reduction</b> .....                 | 3  |
| <b>5.0</b> <b>Survey Results</b> .....                         | 3  |
| <b>5.1</b> <b>Terrestrial Exposure Rate Contour Maps</b> ..... | 3  |
| <b>5.2</b> <b>Exposure Rate Distribution</b> .....             | 3  |
| <b>5.3</b> <b>Gamma Energy Spectra</b> .....                   | 3  |
| <b>5.4</b> <b>Man-Made Gamma Emitters</b> .....                | 13 |
| <b>5.5</b> <b>Ground-Based Measurements Results</b> .....      | 13 |
| <b>5.6</b> <b>Airborne Radon Exposure Rates</b> .....          | 15 |
| <b>6.0</b> <b>Conclusions</b> .....                            | 15 |

## **Figures**

|  |   |
|--|---|
| <b>1</b> <b>MBB BO-105 Helicopter with Detector Pods</b> .....                           | 1 |
| <b>2</b> <b>Mobile Computer Processing Laboratory</b> .....                              | 2 |
| <b>3</b> <b>Exposure Rate Map of the Superconducting Super Collider Laboratory</b> ..... | 4 |
| <b>4</b> <b>Key to the SSCL Exposure Rate Map Subsections</b> .....                      | 5 |
| <b>5</b> <b>Midlothian Subsection of the SSCL Exposure Rate Map</b> .....                | 6 |
| <b>6</b> <b>Waxahachie Subsection of the SSCL Exposure Rate Map</b> .....                | 7 |

|    |  |    |
|----|--|----|
| 7  | Palmer Subsection of the SSCL Exposure Rate Map .....          | 8  |
| 8  | Maypearl Subsection of the SSCL Exposure Rate Map .....        | 9  |
| 9  | Avalon Subsection of the SSCL Exposure Rate Map .....          | 10 |
| 10 | Ennis Subsection of the SSCL Exposure Rate Map .....           | 11 |
| 11 | East Ennis Subsection of the SSCL Exposure Rate Map .....      | 12 |
| 12 | Exposure Rate Frequency Distribution .....                     | 13 |
| 13 | Terrestrial Gamma-Energy Spectrum over Waxahachie, Texas ..... | 13 |

## Tables

|     |   |    |
|-----|---|----|
| 1   | Aerial Gamma System Minimum Detectable Activities ..... | 14 |
| 2   | Radioactive Isotope Concentration in the Soil .....     | 14 |
| 3   | Aerial and Ground-Based Exposure Rate Comparison .....  | 15 |
| C-1 | Ground-Based Measurement Site Descriptions .....        | 20 |

## Appendix

|   |  |    |
|---|--|----|
| A | SSCL Survey Parameters .....                     | 17 |
| B | General Data Analysis Methods .....              | 18 |
| C | Ground-Based Measurement Site Descriptions ..... | 20 |
|   | References .....                                 | 22 |

## 1.0 INTRODUCTION

An aerial radiological gamma survey was conducted over the Superconducting Super Collider Laboratory (SSCL), Waxahachie, Texas, from July 22 through August 20, 1991. The survey was performed by EG&G Energy Measurements, Inc. (EG&G/EM) of Las Vegas, Nevada, and sponsored by the United States Department of Energy (DOE). EG&G/EM, a prime contractor to the DOE, has conducted radiological surveys for the DOE, the Nuclear Regulatory Commission (NRC), and other U.S. government agencies for more than thirty years.

The purpose of the survey was to map the background terrestrial gamma exposure rates in the 1,036 square kilometers (400 square miles) of the site. The survey area included the interior of the accelerator ring, which is 85 kilometers in circumference (53 miles), and the area extending at least 3 kilometers (2 miles) beyond the ring. A uniform set of parallel lines was flown at 305-meter intervals (1,000 feet) to achieve coverage of the area.

A gamma exposure rate map has been derived from the aerial data as an indicator of the terrestrial exposure at 1 meter above the ground. A search of the data was conducted for man-made gamma emitters, but none were found.

Exposure rates and soil samples were acquired at 14 locations on the SSCL site. These ground-based data have been compared to the aerial data.

## 2.0 SURVEY SITE DESCRIPTION

The SSCL extends from 29 kilometers (18 miles) to 60 kilometers (37 miles) south of Dallas, Texas, and lies entirely within Ellis County. The predominant cities in the area are Waxahachie, the Ellis county seat, which lies within 8 kilometers (5 miles) of the center of the site, and Ennis, on the southeast perimeter. Basic industry operates in both Waxahachie and Ennis.

At the time of the survey, land acquisition was still in process for this giant undertaking and construction of laboratory buildings had just begun. The Magnet Development Laboratory, southwest of Waxahachie,

was nearly complete, and some experimental tunneling was in progress.

A weathered escarpment runs north-south on the west side of the site. Elevations decrease from about 262 meters (860 feet) above mean sea level (MSL) in the northwest near Cedar Hill, Texas, to about 122 meters (400 feet) in the southeast. A number of small streams drain toward the southeast into the Trinity River, 16.1 kilometers (10 miles) west of the site. An array of earthen dams controls flooding and erosion and yields irrigation water.

Animal husbandry, dairies, and row crops dominate in this intensively farmed area. Most of the land has been cleared, with little woodland remaining except on the escarpment in the west.

## 3.0 SURVEY EQUIPMENT AND METHODS

### 3.1 Aircraft System

A Messerschmitt-Bolkow-Blohm (MBB) BO-105 helicopter was used as the aerial platform (Figure 1). The aircraft carried two detector pods, each containing four 2-in  $\times$  4-in  $\times$  16-in log-type NaI(Tl) gamma detectors.



FIGURE 1. MBB BO-105 HELICOPTER WITH DETECTOR PODS

Gamma signals originating in the NaI(Tl) detectors were routed to the Radiation and Environmental Data Acquisition and Recorder (REDAR IV) system for conversion and storage on magnetic tape. Pressure, temperature, and radar altitude transducer data were also acquired and stored by the REDAR. Real-time gamma energy spectra, total gamma count rates, and

other data were output to a small CRT screen for the system operator.

The aircraft pilot was guided over the programmed flight lines by an indicator that derives its signal from the triangulation of two ultrahigh-frequency (UHF) transponders\* on the ground and a master unit in the aircraft. These position data were also stored by the REDAR.

### 3.2 Data Van

A minicomputer-based system (Figure 2) housed in a van was used during the survey to evaluate the aerial data immediately following each survey flight. The system contains hardware and software that operate on the survey data stored on magnetic tape. The system operator can plot both gamma energy spectra from any portion of the gamma survey and count-rate isopleths scaled to a map or photograph. In this manner, the intensity and location of the isotope emitters can be identified.

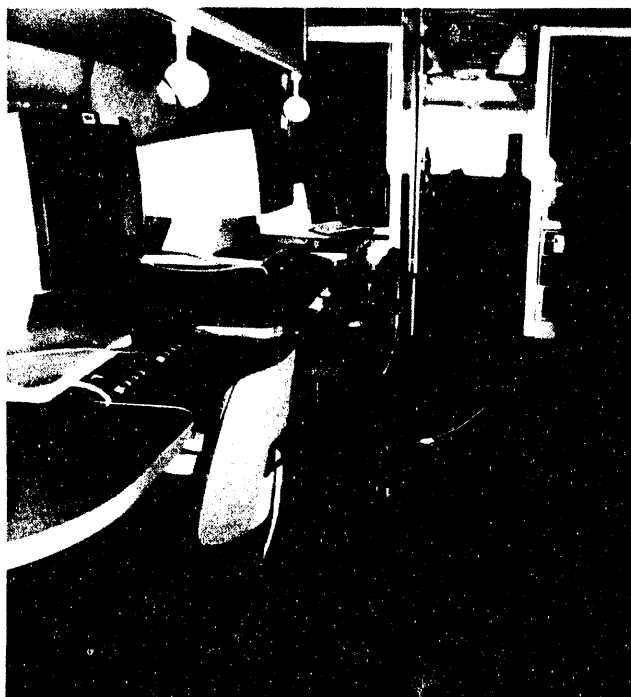


FIGURE 2. MOBILE COMPUTER PROCESSING LABORATORY

\* A second set of transponders operating at a much higher frequency than the first set was used also, but at a later stage of the survey.

### 3.3 Survey Method

A standardized procedure for aerial gamma surveys was followed during the survey of the SSCL. Steps in the procedure are as follow:

- A. Two UHF transponders were placed outside the survey area. The transponder locations and the center of the survey area form an approximate equilateral triangle.
- B. A perimeter flight of roads in the survey area was then made. The transponder data from this flight were used to scale distances to a road map of the survey area. In this way, each subsequent gamma datum could be plotted accurately (within about 9 meters) on the map.
- C. A test line, just south of Cleburne, and a water line, southwest of Cleburne, were located. Gamma data versus altitude over the test line and water line were examined and compared to the Las Vegas calibration line beside Lake Mead.
- D. Following the perimeter and test line flights, routine survey flights began. All survey lines were flown at an altitude of 91 meters (300 feet). Each flight, preceded by a preflight in which the system was calibrated and the data tape analyzed for proper system operation, consisted of:
  1. A pass over the test line and the water line at survey altitude.
  2. Passes in an east-west direction following preprogrammed adjacent lines over the survey area.
  3. A repeat pass over the test line and the water line.
- E. Following each survey flight, the data were reduced to engineering units by a standard computer program. These were examined by the survey scientist and data technician for integrity and quality. The reduced data were extrapolated to 1 meter above the ground, and a contour map was drawn in units of exposure rate. In addition, a contour map was also drawn from an algorithm designed to show possible man-made gamma activity. The survey parameters are listed in Appendix A.

### 3.4 Ground-Based Measurements

Exposure rate measurements, high purity germanium spectral measurements, and soil samples were

obtained at 14 locations during the SSCL survey. These measurements were made to support the integrity of the aerial results. A Reuter-Stokes pressurized ionization chamber was used for each exposure measurement at a height of 1 meter at the center of a measurement area 183 meters (600 feet) in diameter. Soil samples, to a depth of 15 centimeters, were also obtained at the center and at four points of the compass on the circumference of the circular area. The soil samples were dried and their gamma activities measured on a germanium-based detector system at the EG&G/EM Santa Barbara Laboratory.<sup>1,2</sup>

#### 4.0 GENERAL DATA REDUCTION

Two primary methods are used to evaluate the gamma fluence rate measurements made with the aerial system's NaI(Tl) detectors. The first is the gross count (GC) technique which is used to determine exposure rate, and the second is the spectral window technique which is used to measure concentrations of specific nuclides. These are described in Appendix B.

#### 5.0 SURVEY RESULTS

The principal results of the aerial survey and analysis are the terrestrial exposure rate contour maps of the Superconducting Super Collider area. These represent gamma exposure rates at 1 meter above ground level (AGL) due to gamma emitting isotopes in the soil. The aerial results are compared to ground-based measurements and a typical gamma energy spectrum over Waxahachie is shown. A search of the aerial data for man-made isotopes (Appendix B) produced a negative result though ground-based measurements indicated some international fallout.

##### 5.1 Terrestrial Exposure Rate Contour Maps

The exposure rate contour map of the entire survey area is shown in Figure 3. Contour intervals are at 2 microroentgens per hour ( $\mu\text{R}/\text{h}$ ) except for the lowest interval which is from 0 to 1  $\mu\text{R}/\text{h}$ . The terrestrial exposure rate will approach zero at the center of Lake

Waxahachie and Bardwell Lake although a zero level is not shown. Statistical uncertainties in counting and in airborne radon concentrations give the zero contour a mottled effect with little value. Thus, the first or lowest contour is chosen at 1  $\mu\text{R}/\text{h}$  and generally occurs over the water of the large lakes.

The range of terrestrial exposure rates extends from about zero to nearly 9  $\mu\text{R}/\text{h}$ . The variable concentrations of natural radioactive isotopes are attributable to topographical differences. The hills on the western half of the map indicate a more complex geologic structure than that shown on the eastern half.

Figure 4 is the key to the location of each subsection. The large area exposure rate map has been divided into seven subsections shown in Figures 5 through 11. These underlying maps are portions of the United States Geological Survey 1:24,000 contour maps.

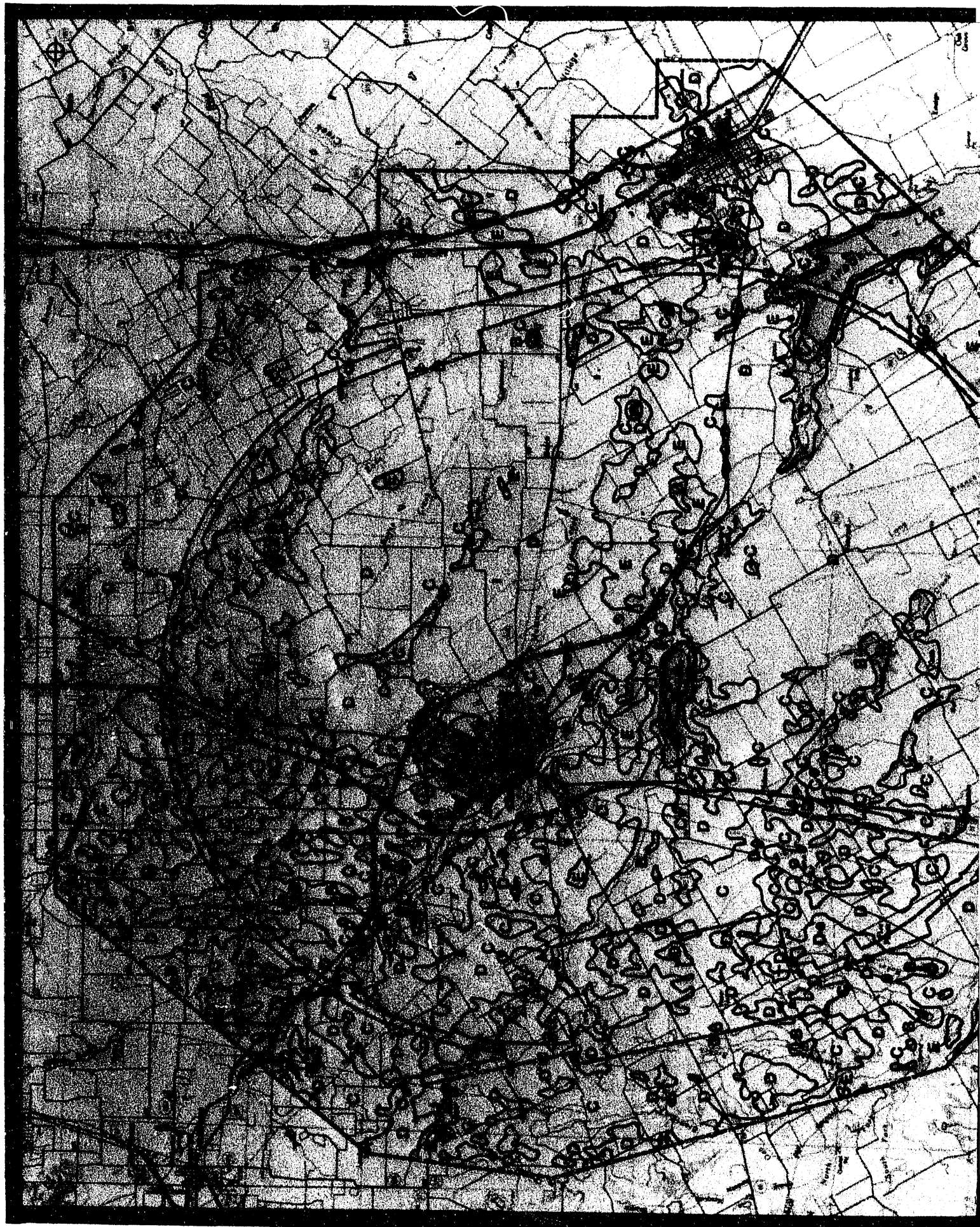
##### 5.2 Exposure Rate Distribution

The exposure rate frequency distribution for the entire area is shown in Figure 12. All of the 70,000 data points from the 3,392 kilometers (2,108 miles) of flight line are represented. These data are plotted for each 1  $\mu\text{R}/\text{h}$  interval and at the mean exposure rate in each interval. The mean exposure rate in the survey area is 5.4  $\mu\text{R}/\text{h}$ , and the most probable exposure rate is 5.9  $\mu\text{R}/\text{h}$ . Fifty percent of the measured values lie within 0.9  $\mu\text{R}/\text{h}$  of the most probable value, *i.e.*, between 5  $\mu\text{R}/\text{h}$  and 6.8  $\mu\text{R}/\text{h}$ .

The geographic distributions show larger mean exposure rates in the eastern half of the survey area than in the western half. The mean value west from Waxahachie is 4.9  $\mu\text{R}/\text{h}$ , and from Waxahachie to the east it is 5.8  $\mu\text{R}/\text{h}$ . The width of the exposure rate frequency distribution is wider in the west than in the east, as one might expect, because of the hills in the west and the flat, uniform terrain in the east.

##### 5.3 Gamma Energy Spectra

Gamma energy spectra, accumulated at the rate of one each second, are used to identify the particular



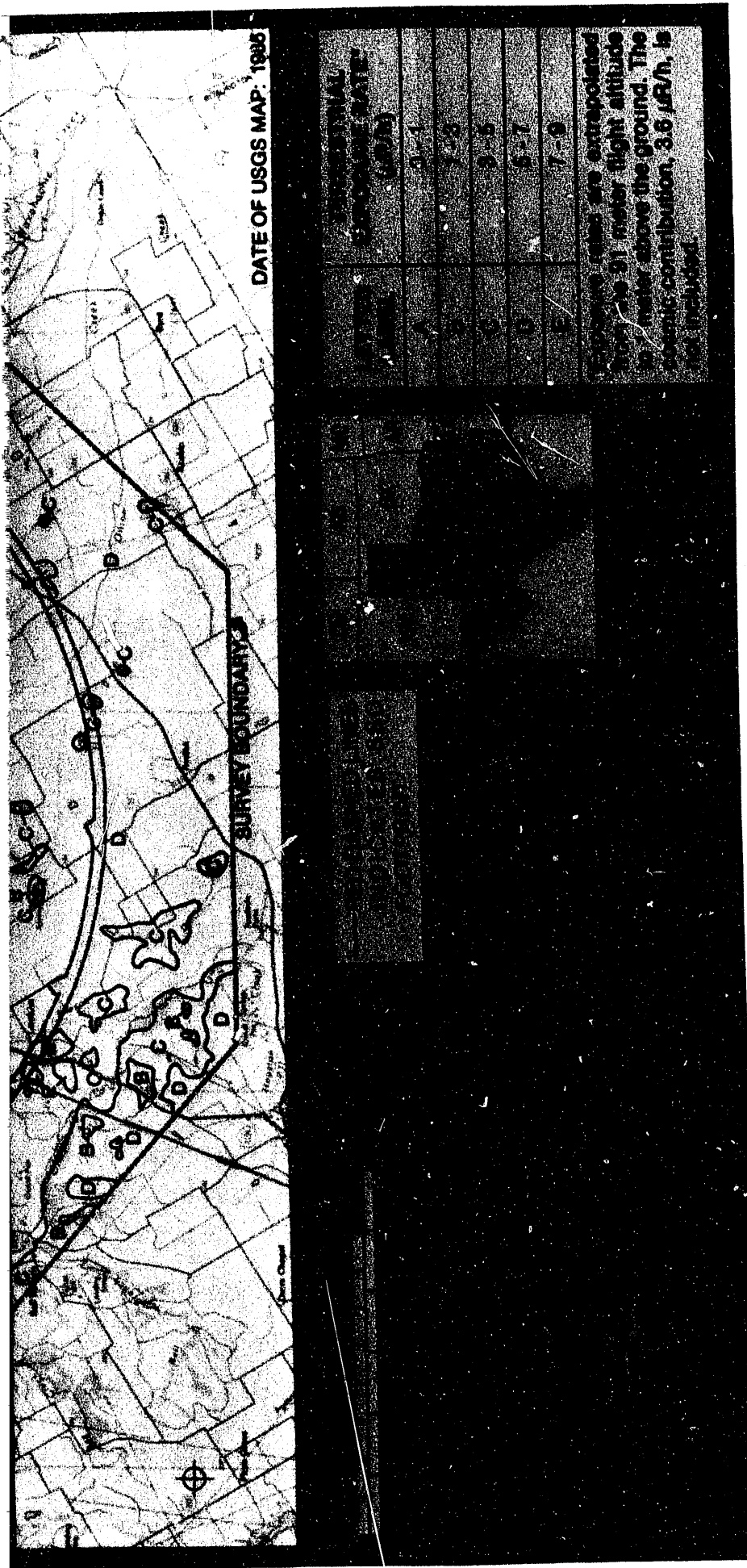
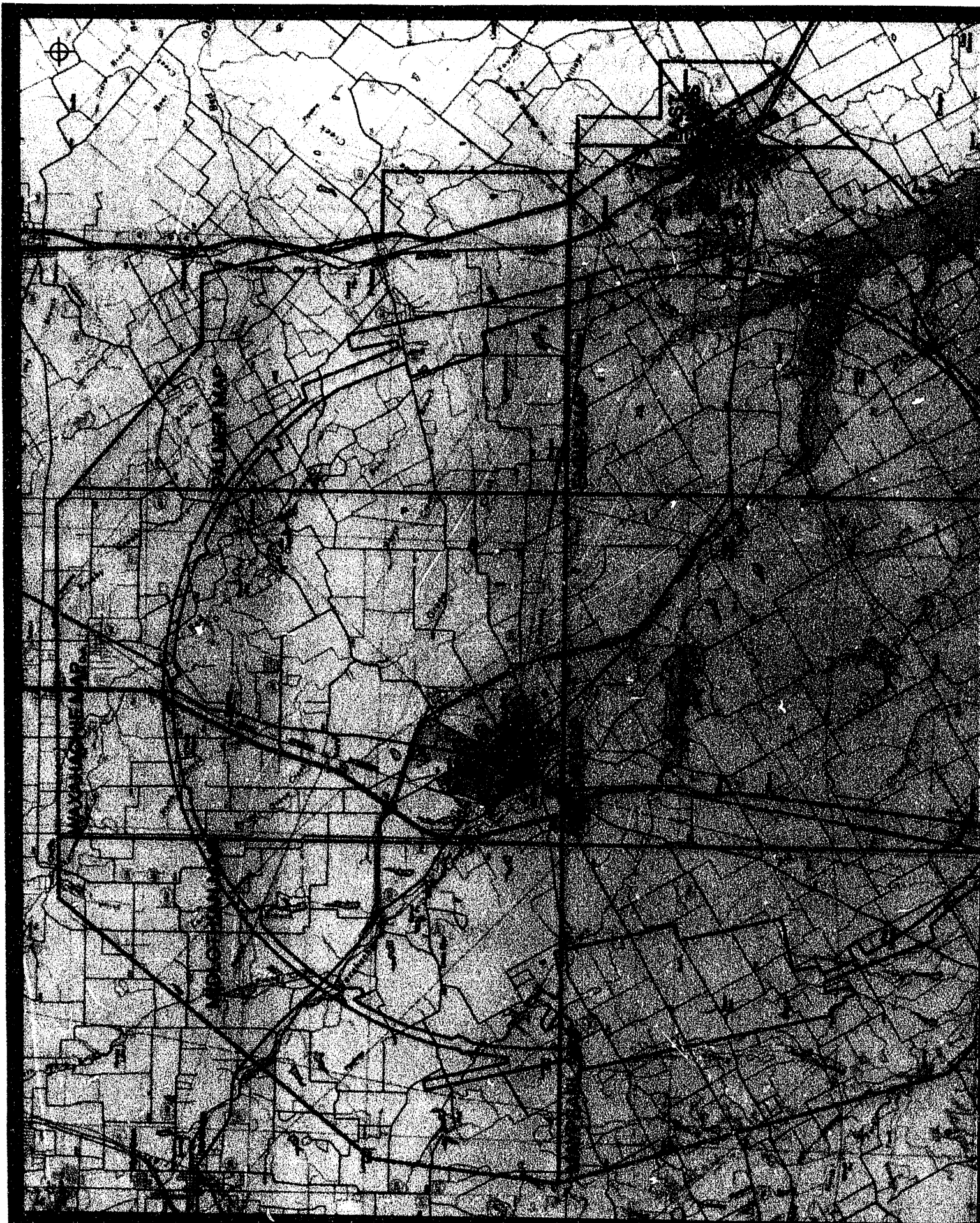
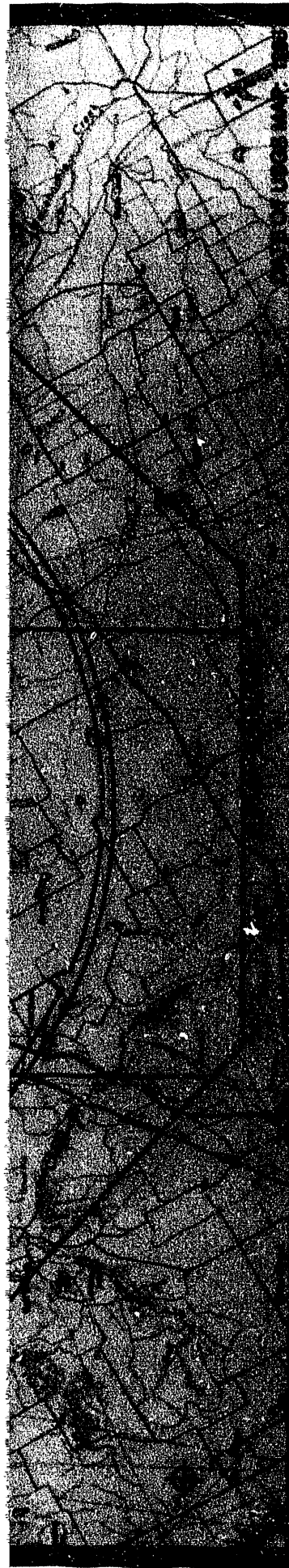


FIGURE 3. *EXPOSURE RATE MAP OF THE SUPERCONDUCTING SUPER COLLIDER LABORATORY*





**FIGURE 4. KEY TO THE SSCL EXPOSURE RATE MAP SUBSECTIONS**

Legend for Figure 4: The SSCL exposure rate map is divided into 100 numbered subsections. The following key identifies the symbols used in the map:

1. Solid black area: 100% exposure rate (highest level).

2. White area: 0% exposure rate (lowest level).

3. Hatched area: 50% exposure rate.

4. Dashed area: 25% exposure rate.

5. Dotted area: 10% exposure rate.

6. Cross-hatched area: 75% exposure rate.

7. Vertical lines: 50% exposure rate.

8. Horizontal lines: 25% exposure rate.

DATE OF USGS MAP: 1978

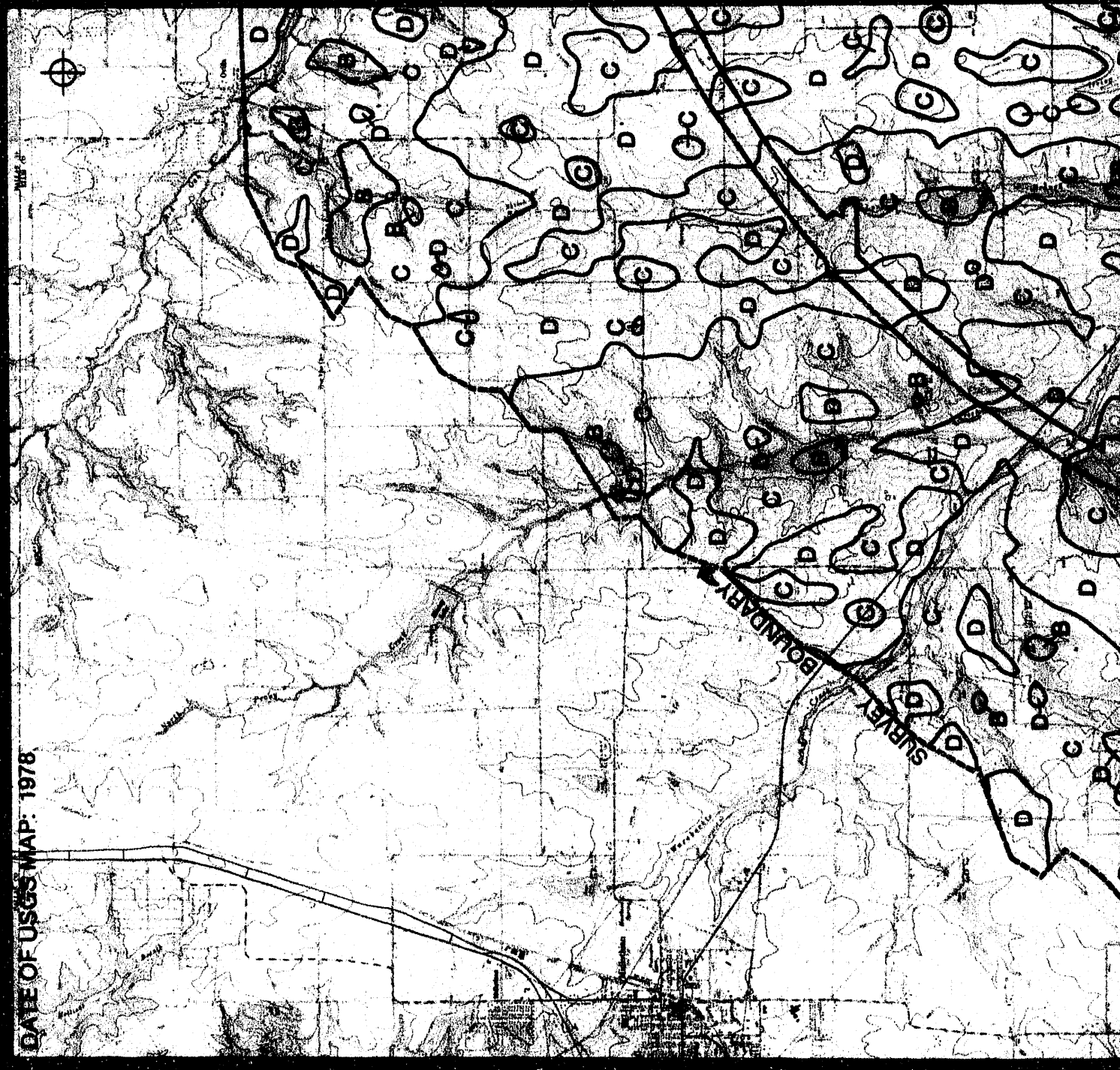
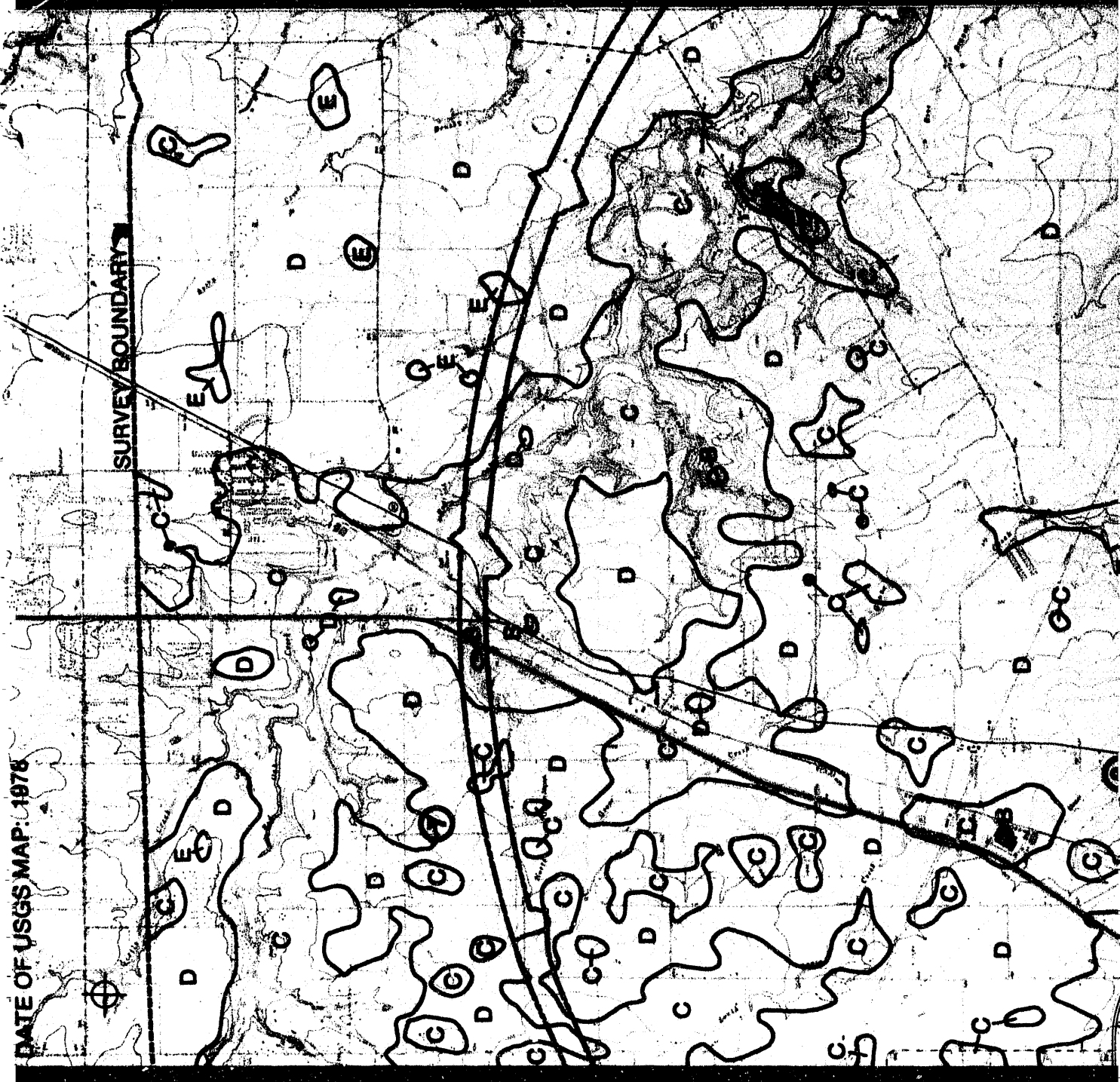




FIGURE 5. MIDLOTHIAN SUBSECTION OF THE SSCL EXPOSURE RATE MAP



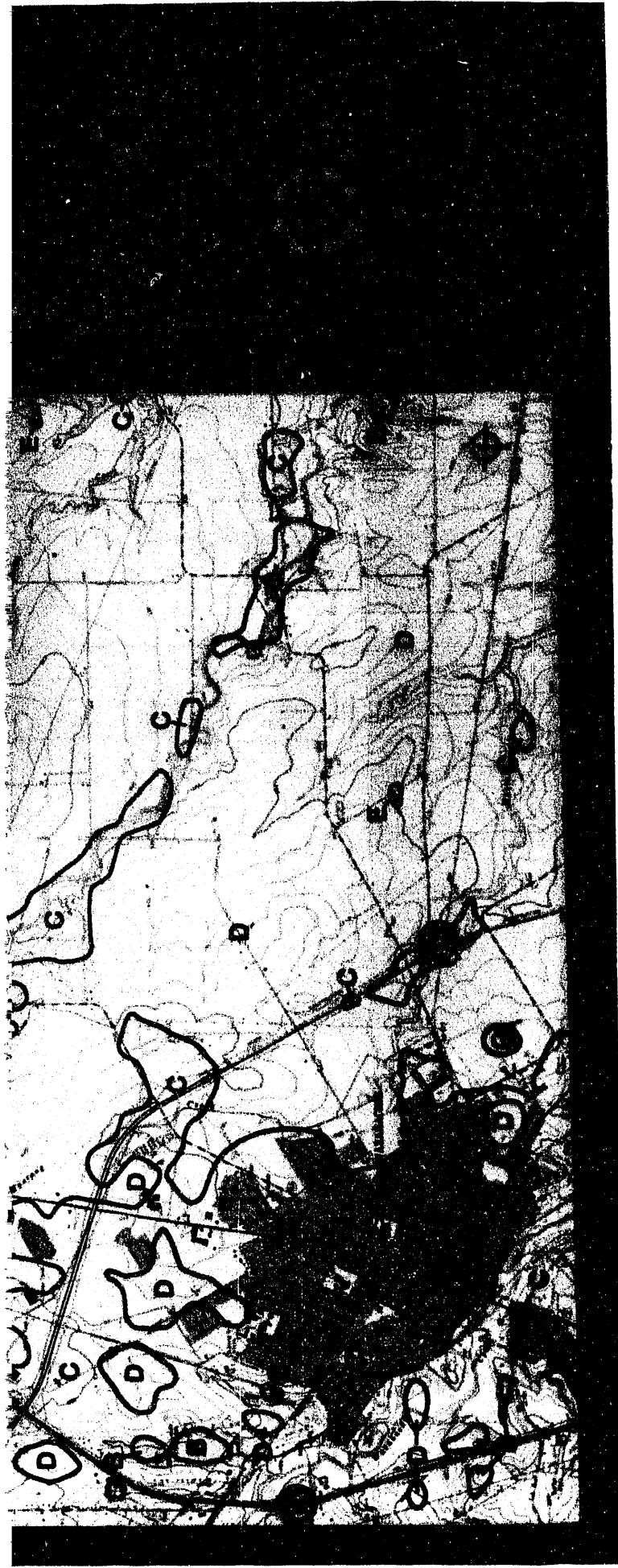


FIGURE 6. WAXAHACHIE SUBSECTION OF THE SSCL EXPOSURE RATE MAP





FIGURE 7. PALMER SUBSECTION OF THE SSCL EXPOSURE RATE MAP

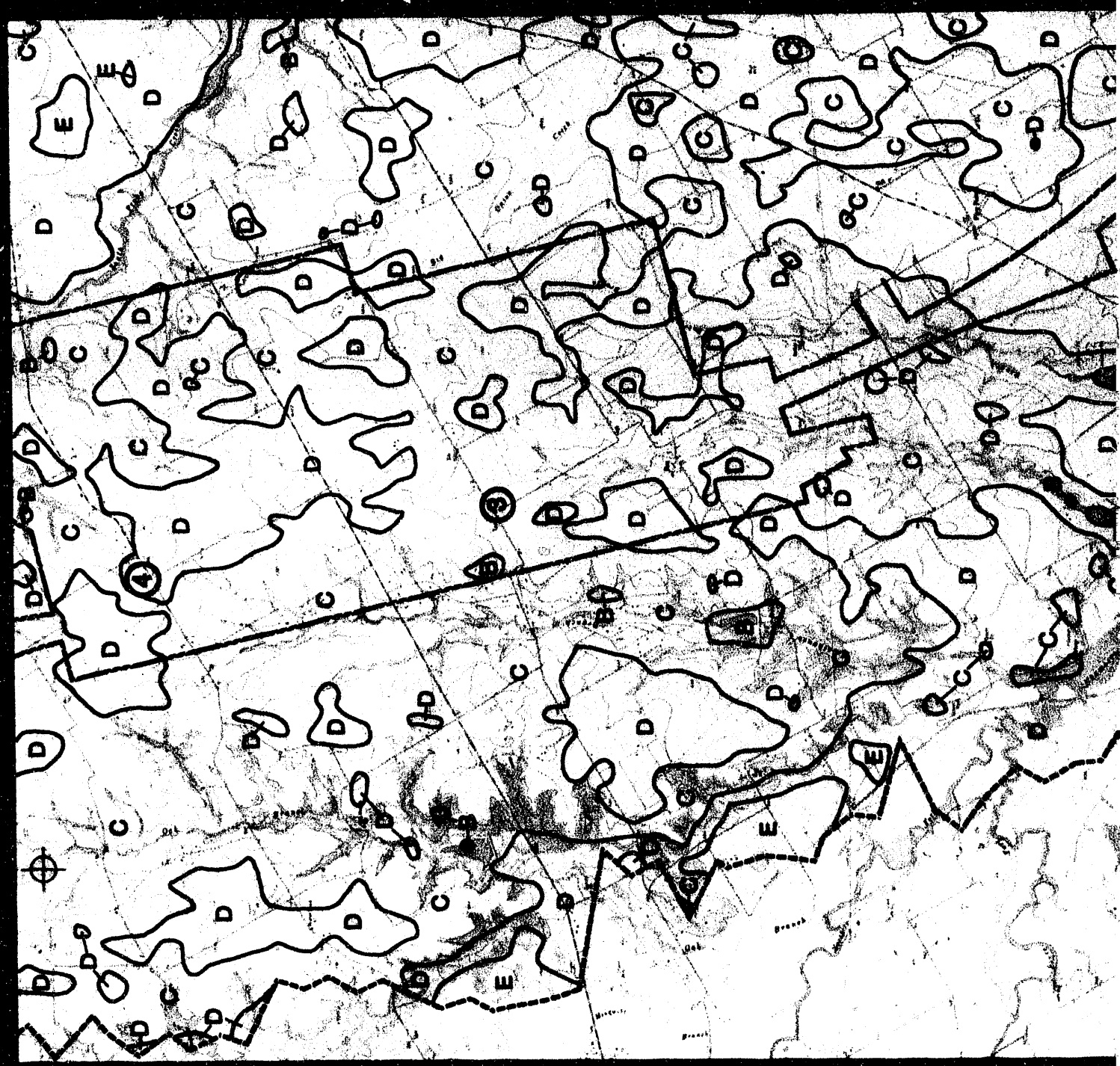




FIGURE 8. MAYPEARL SUBSECTION OF THE SSCL EXPOSURE RATE MAP





FIGURE 9. AVALON SUBSECTION OF THE SSCL EXPOSURE RATE MAP

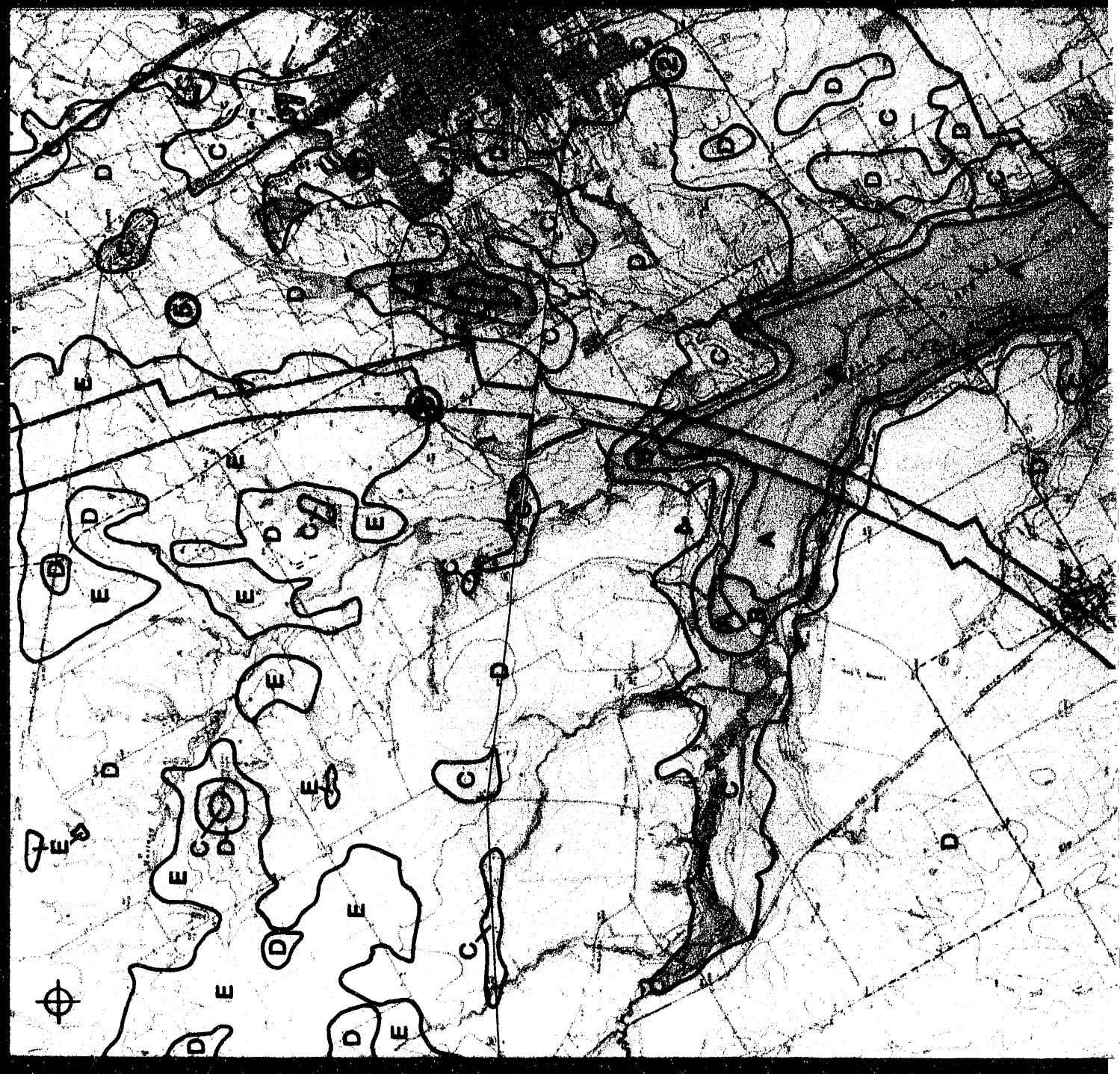
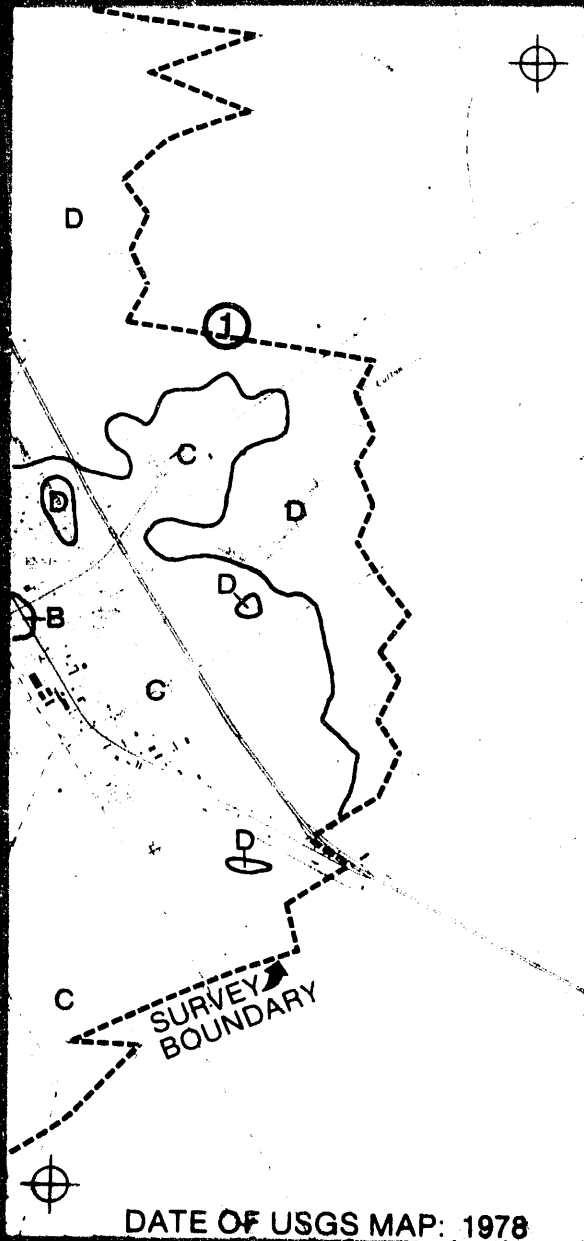




FIGURE 10. ENVIS SUBSECTION OF THE SSCL EXPOSURE RATE MAP



| CONVERSION RATE |   |
|-----------------|---|
| LETTER LABEL    | TERRESTRIAL EXPOSURE RATE* ( $\mu\text{R}/\text{h}$ ) |
| B               | 1 - 3   |
| C               | 3 - 5   |
| D               | 5 - 7   |

\*Exposure rates are extrapolated from the 91 meter flight altitude to 1 meter above the ground. The cosmic contribution,  $3.6 \mu\text{R}/\text{h}$ , is not included.

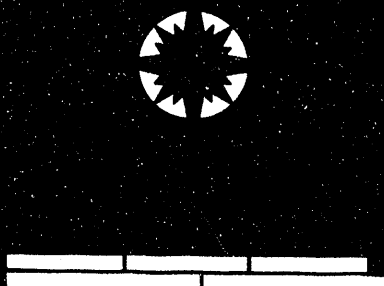
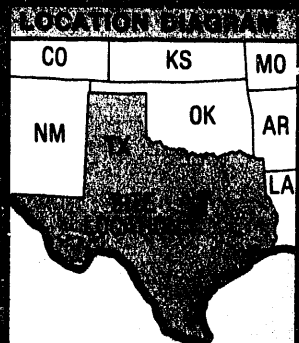


FIGURE 11 EAST ENNIS SUBSECTION OF THE SSCL EXPOSURE RATE MAP

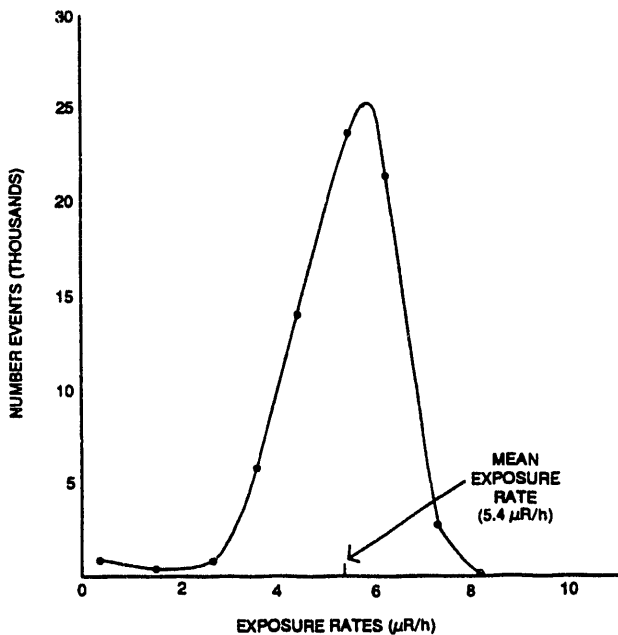


FIGURE 12. EXPOSURE RATE FREQUENCY DISTRIBUTION

radionuclides that contribute to the gamma exposure. Figure 13 is the gamma energy spectrum accumulated over Waxahachie, Texas. The peaks in the energy spectrum identify only natural gammas that have originated in the soil, buildings, and other materials in Waxahachie. Visible peaks in the spectrum identify only natural radioactive potassium ( $^{40}\text{K}$ ), uranium daughters bismuth-214 ( $^{214}\text{Bi}$ ) and lead-214 ( $^{214}\text{Pb}$ ), and thorium daughters thallium-208 ( $^{208}\text{Tl}$ ) and actinium-228 ( $^{228}\text{Ac}$ ).

#### 5.4 Man-Made Gamma Emitters

A search was made of all the aerial gamma data for man-made radioactivity. Most fission and activation isotopes emit gammas and may be detected at some minimum activity level by the aerial gamma measuring system. The search method, the man-made gross count (MMGC) algorithm as outlined in Appendix B, yielded no measurable man-made gamma activity in the entire 400-square-mile survey area. Man-made radioactivity may exist, though at activities below the minimum detectable levels for the aerial system. Also, buried or shielded radioactivity may not be detected. Table 1 lists a few minimum detectable activities (MDA) for fission and neutron activation products.

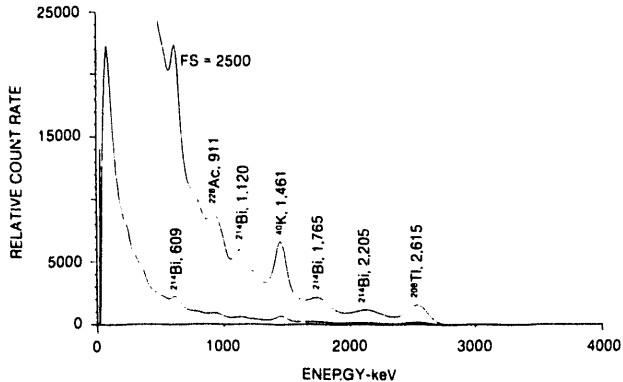


FIGURE 13. TERRESTRIAL GAMMA ENERGY SPECTRUM OVER WAXAHACHIE, TEXAS

Finally, no attempt has been made in this report to map the very low levels of cesium-137 ( $^{137}\text{Cs}$ ), an international fallout fission product. This isotope occurs nearly everywhere in the northern hemisphere at or below the MDA of the aerial gamma system. Concentrations of  $^{137}\text{Cs}$  would be found in the MMGC search method discussed above and in Appendix B.

#### 5.5 Ground-Based Measurements Results

Ion chamber measurements and soil samples were collected at fourteen sites in and near the SSCL area during the survey. The soil samples were evaluated for moisture and radioactive isotope content in EG&G/EM's laboratory in Santa Barbara, California.<sup>1,2</sup> The results are given in Table 2. The measurement locations are numbered on the exposure rate contour maps, presented in Figures 5 through 11. Soil samples were not collected at Location 11 (the lawn of the Ellis County court house) to avoid disfiguring this landmark. Collection time, date, and coordinates, as well as a short description of each site are given in Appendix C.

From the soil sample activity results, a terrestrial exposure rate of 1 meter above the ground may be computed. Adding a cosmic contribution<sup>3</sup> of 3.6  $\mu\text{R/h}$  to these computed values yields the majority of the exposure, terrestrial plus cosmic, at 1 meter above the ground. These values, along with the ion chamber measurement and the aerial measurement over each ground location, are listed in Table 3. The aerial terrestrial measurement also has a 3.6  $\mu\text{R/h}$  cosmic component added, whereas the ion chamber measures both the terrestrial and cosmic components.

**Table 1. Aerial Gamma System Minimum Detectable Activities**

| Isotope           | Energy (keV) | Large Area Surface Source ( $\mu\text{Ci}/\text{m}^2$ ) | Large Area Source In Soil <sup>a</sup> ( $\mu\text{Ci}/\text{m}^2$ ) | Point Source A <sup>b</sup> (mCi) | Point Source B <sup>c</sup> (mCi) |
|-------------------|--------------|---|--|-----------------------------------|-----------------------------------|
| $^{60}\text{Co}$  | 1173, 1333   | 0.04  | 0.095  | 1.6                               | 10                                |
| $^{137}\text{Cs}$ | 662          | 0.08  | 0.26   | 3.8                               | 25                                |
| $^{235}\text{U}$  | 185          | 0.22  | 0.76   | 4.9                               | 80                                |

<sup>a</sup> The large area source in soil is assumed to be exponentially distributed with depth of the form:

$$\text{Concentration} = \text{Co} \cdot e^{(-\text{depth}/10 \text{ cm})}$$

<sup>b</sup> The point source A is assumed to be under the path of the aircraft.

<sup>c</sup> The point source B is assumed to lie at 500 feet to the side of the aircraft path, *i.e.*, centered between two flight lines at SSCL.

**Table 2. Radioactive Isotope Concentration in the Soil<sup>a</sup>**

| Location | % Moisture (%) <sup>b</sup> | $^{226}\text{Ra}$ (pCi/g) <sup>b</sup> | $^{232}\text{Th}$ (pCi/g) <sup>b</sup> | $^{137}\text{Cs}$ (pCi/g) <sup>b</sup> | $^{40}\text{K}$ (pCi/g) <sup>b</sup> |
|----------|-----------------------------|--|--|--|--------------------------------------|
| 1        | $15 \pm 2$                  | $0.9 \pm 0.1$                          | $0.9 \pm 0.1$                          | $0.5 \pm 0.1$                          | $7.3 \pm 0.5$                        |
| 2        | $13 \pm 3$                  | $0.9 \pm 0.1$                          | $0.8 \pm 0.1$                          | $0.3 \pm 0.1$                          | $7.3 \pm 0.7$                        |
| 3        | $21 \pm 2$                  | $1.3 \pm 0.1$                          | $0.7 \pm 0.1$                          | $0.4 \pm 0.2$                          | $5.8 \pm 1.0$                        |
| 4        | $23 \pm 2$                  | $1.6 \pm 0.4$                          | $1.5 \pm 0.05$                         | $0.3 \pm 0.1$                          | $11 \pm 1.0$                         |
| 5        | $18 \pm 2$                  | $1.0 \pm 0.1$                          | $1.2 \pm 0.1$                          | $0.2 \pm 0.05$                         | $8.4 \pm 0.8$                        |
| 6        | $21 \pm 2$                  | $1.2 \pm 0.2$                          | $1.6 \pm 0.1$                          | $0.2 \pm 0.06$                         | $14.5 \pm 1$                         |
| 7        | $16 \pm 2$                  | $0.9 \pm 0.2$                          | $0.7 \pm 0.2$                          | $0.6 \pm 0.2$                          | $7.5 \pm 13$                         |
| 8        | $19 \pm 1$                  | $1.0 \pm 0.2$                          | $1.1 \pm 0.1$                          | $0.15 \pm .06$                         | $6.3 \pm 0.4$                        |
| 9        | $16 \pm 1$                  | $1.5 \pm 0.2$                          | $1.3 \pm 0.05$                         | $0.12 \pm .05$                         | $5.3 \pm 0.3$                        |
| 10       | $12 \pm 3$                  | $1.1 \pm 0.2$                          | $0.8 \pm 0.2$                          | $0.28 \pm .09$                         | $4.4 \pm 1.4$                        |
| 12       | $12 \pm 3$                  | $1.1 \pm 0.1$                          | $1.2 \pm 0.2$                          | $0.27 \pm .03$                         | $7 \pm 2$                            |
| 13       | $11 \pm 1$                  | $1.0 \pm 0.2$                          | $0.7 \pm 0.2$                          | $0.05 \pm .03$                         | $3.6 \pm 0.9$                        |
| 14       | $15 \pm 3$                  | $1.1 \pm 0.2$                          | $1.0 \pm 0.2$                          | $0.34 \pm 0.1$                         | $7 \pm 1$                            |

<sup>a</sup> Concentrations are for dried soil samples.

<sup>b</sup> Concentration uncertainties are at the one standard deviation level.

Examination of these exposure rate sets shows fair agreement. Seven of these locations are in open areas without extensive buildings and roads. These

are Locations 3, 5, 6, 7, 8, 9, and 12. The average exposures for these locations from the soil sample, ion chamber, and aerial results are  $9.1 \mu\text{R}/\text{h}$ ,  $8.2 \mu\text{R}/\text{h}$ ,

and 9.4  $\mu\text{R}/\text{h}$  respectively. The aerial and soil sample average results agree very well, while the ion chamber average is about 1  $\mu\text{R}/\text{h}$  smaller.

There are a number of reasons why ground-based measurements may differ from aerial measurements:

- A. The aerial system measures a much larger area (several hectares) than ground-based data (about 1 hectare).
- B. The aircraft did not fly directly over the ground measurement sites.
- C. The ground data were taken during the aerial survey, but on different days for specific locations. Therefore, soil moisture may have changed between the time of each ground-based measurement or sample and the time of the aerial measurement. Changing soil moisture changes the exposure rate.<sup>4</sup>

## 5.6 Airborne Radon Exposure Rates

The contribution of airborne radon daughters (principally  $^{214}\text{Bi}$  and  $^{214}\text{Pb}$ ) to the exposure rate at 1 meter

has not been evaluated in the tables above. The aerial measurement utilizes over-water data during each flight to reduce aerial radon errors to about 0.1  $\mu\text{R}/\text{h}$  at 1 meter, but the ion chamber measures the radon in the air as well as in the ground. The radon and its daughters are at equilibrium with radon-226 ( $^{226}\text{Ra}$ ) when the soil samples are counted. From the aerial over-water data (48 measurements), estimates of minimum and maximum radon daughter contributions to exposure are zero to 0.4  $\mu\text{R}/\text{h}$ .

## 6.0 CONCLUSIONS

An aerial terrestrial gamma survey conducted at 91 meters above the area occupied by the Superconducting Super Collider Laboratory in Ellis County, Texas, shows nominal background gamma exposure levels. The gamma exposure rate due to natural radioactivity in the soil at 1 meter above the ground averages about 5.4  $\mu\text{R}/\text{h}$ . The gamma exposure rate map of this area shows an exposure rate 1  $\mu\text{R}/\text{h}$  larger in the eastern half of the area than in the western half.

A detailed examination of the 70,000 aerial data points yielded no evidence of man-made gammas, i.e., X rays or radiation therapy gamma sources.

Table 3. Aerial and Ground-Based Exposure Rate Comparison

| Location Number | Estimate from Soil Analysis <sup>a,b</sup> ( $\mu\text{R}/\text{h}$ ) | Ion Chamber Measurement <sup>c,d</sup> ( $\mu\text{R}/\text{h}$ ) | Estimate from Aerial Data <sup>b,e</sup> ( $\mu\text{R}/\text{h}$ ) |
|-----------------|---|---|---|
| 1               | 8.3 $\pm$ 0.7   | f   | f   |
| 2               | 8.1 $\pm$ 1.0   | f   | 8.5   |
| 3               | 7.8 $\pm$ 0.6   | 7.2   | 8.0   |
| 4               | 10.6 $\pm$ 0.8  | (6-12)  | 9.1   |
| 5               | 9.1 $\pm$ 0.8   | 8.4   | 9.8   |
| 6               | 10.9 $\pm$ 0.8  | 9.4   | 11.1  |

<sup>a</sup> The soil sample estimates include the effect of soil moisture.

<sup>b</sup> A cosmic exposure component of 3.6  $\mu\text{R}/\text{h}$  has been added to the soil sample and to the aerial terrestrial components.

<sup>c</sup> The uncertainty in the ion chamber measurement is about 1.0  $\mu\text{R}/\text{h}$ .

<sup>d</sup> The airborne radon component is measured by the ion chamber only, and no radon exposure rate estimate has been added to the soil sample or the aerial values.

<sup>e</sup> The uncertainty in the aerial measurement is about 1.0  $\mu\text{R}/\text{h}$ .

<sup>f</sup> Four omissions in the table show the absence of the original sample.

**Table 3. Aerial and Ground-Based Exposure Rate Comparison (continued)**

| Location Number | Estimate from Soil Analysis <sup>a,b</sup> ( $\mu\text{R/h}$ ) | Ion Chamber Measurement <sup>c,d</sup> ( $\mu\text{R/h}$ ) | Estimate from Aerial Data <sup>b,e</sup> ( $\mu\text{R/h}$ ) |
|-----------------|--|--|--|
| 7               | 7.9 $\pm$ 1.0  | 7.0  | 8.8  |
| 8               | 8.7 $\pm$ 0.8  | 8.0  | 8.9  |
| 9               | 9.9 $\pm$ 0.6  | 8.8  | 9.4  |
| 10              | 9.1 $\pm$ 1.4  | 7.2  | 8.2  |
| 11              | f  | 9.6  | 6.7  |
| 12              | 9.6 $\pm$ 1.3  | 8.8  | 9.9  |
| 13              | 7.4 $\pm$ 1.2  | 7.2  | 8.6  |
| 14              | 8.8 $\pm$ 1.3  | 8.0  | 7.1  |

<sup>a</sup> The soil sample estimates include the effect of soil moisture.

<sup>b</sup> A cosmic exposure component of 3.6  $\mu\text{R/h}$  has been added to the soil sample and to the aerial terrestrial components.

<sup>c</sup> The uncertainty in the ion chamber measurement is about 1.0  $\mu\text{R/h}$ .

<sup>d</sup> The airborne radon component is measured by the ion chamber only, and no radon exposure rate estimate has been added to the soil sample or the aerial values.

<sup>e</sup> The uncertainty in the aerial measurement is about 1.0  $\mu\text{R/h}$ .

<sup>f</sup> Four omissions in the table show the absence of the original sample.

## APPENDIX A

### SSCL SURVEY PARAMETERS

|                                 |   |
|---------------------------------|---|
| <b>Survey Site:</b>             | Superconducting Super Collider Laboratory,<br>Waxahachie, Texas   |
| <b>Survey Date:</b>             | July 22 through August 20, 1991   |
| <b>Aircraft:</b>                | MBB BO-105 helicopter   |
| <b>Altitude:</b>                | 91 meters (300 feet) above the ground   |
| <b>Speed:</b>                   | 46 meters per second (90 knots)   |
| <b>Line Spacing:</b>            | 305 meters (1,000 feet)   |
| <b>Line Length:</b>             | 12.9 to 38 kilometers (8 to 23.6 miles)   |
| <b>Line Direction:</b>          | East-West   |
| <b>Number of Lines:</b>         | 121   |
| <b>Detector Array:</b>          | Eight 2-in $\times$ 4-in $\times$ 16-in NaI(Tl) detectors<br>and two 2-in $\times$ 4-in $\times$ 4-in NaI(Tl) detectors |
| <b>Data Acquisition System:</b> | REDAR IV  |
| <b>Data Acquisition Rate:</b>   | Once per second   |
| <b>Ranging System:</b>          | Both the URS (~425 MHz) and the<br>MRS (~9.3 GHz) were used   |

## APPENDIX B

### GENERAL DATA ANALYSIS METHODS

A few useful methods to treat gamma energy spectra as measured by NaI(Tl) are discussed below.

#### Gross Count Rate

The gross count (GC) rate is defined as the integral count in the energy spectrum between 38 keV and 3,026 keV.

$$GC = \sum_{E=38 \text{ keV}}^{3026 \text{ keV}} \text{Energy Spectrum} \quad (\text{B-1})$$

This integral includes all the natural isotope gammas from  $^{40}\text{K}$ ,  $^{238}\text{U}$ , and  $^{232}\text{Th}$  (KUT, the major terrestrial, natural gamma emitters). Other natural contributors to this integral are cosmic rays, aircraft background, and airborne radon daughters.

The response versus altitude of the aerial system to terrestrial gammas has been measured over a documented test line near Las Vegas, Nevada, for which the concentrations of KUT and the 1-meter exposure rates have been measured separately. From this calibration, the terrestrial gross count rate has been associated with the 1-meter exposure rate in micro-roentgens per hour ( $\mu\text{R}/\text{h}$ ) for natural radioactivity. The conversion equation is:

$$E(1m) = \frac{GC(A) - B}{1167} \cdot e^{0.001794} \quad (\text{B-2})$$

where

$E(1m)$  = Exposure rate extrapolated to 1 m AGL ( $\mu\text{R}/\text{h}$ )

$A$  = Altitude in feet  
 $GC(A)$  = Gross count rate at altitude  $A$  (cps)  
 $B$  = Cosmic, aircraft, and radon background (cps)  
 $B$  is obtained from flights over bodies of water, where the terrestrial count rate is absent.

The gross count has been used for many years in the aerial system as a measure of exposure. Its simplicity yields a rapid assessment of the gamma environment.

Anomalous, or non-natural, gamma sources are found from increases in the gross count rate over the natural count rate. However, subtle anomalies are difficult to find using the gross count rate in areas where its magnitude is variable due to, for example, geologic or ground cover changes. Differential energy data reduction methods, as discussed in the next section, are used to increase sensitivity of the aerial system to anomalous gamma emitters.

#### Spectral Windows

The aerial system produces a gamma energy spectrum each second from which the  $GC$  is computed. Generally, the ratio of natural components in any two integral sections (windows) of the energy spectrum will remain nearly constant in any given area:

$$\sum_{E=a}^b ES \Bigg/ \sum_{E=b}^c ES = \text{Constant} = K \quad (\text{B-3})$$

where

$ES$  = Energy Spectrum

$E$  = Energy

$c > b > a$

The window,  $a-b$ , is placed where gamma rays from a man-made emitter would occur in the spectrum. The result of Equation B-3 could be expected to increase over the constant value. This equation is routinely applied in the data reduction software when a search is made for specific isotopes.

$$S = \sum_{E=a}^b ES - K \sum_{E=b}^c ES \quad (B-4)$$

The net signal,  $S$ , is zero unless anomalous gamma rays are measured in the window defined by  $a$  and  $b$ .

Equation B-4 is used to locate specific isotopes by setting  $a$  and  $b$  to enclose the photopeak of the particular gamma from the isotope. For the general case when any man-made isotope is sought,  $a$ ,  $b$ , and  $c$  are set at 38 keV, 1,394 keV, and 3,026 keV respectively. Because most long-lived man-made isotopes emit gammas in this energy range (38 keV to 1,394 keV), Equation B-4 becomes a general search tool and is called the man-made gross count.

## APPENDIX C

### GROUND-BASED MEASUREMENT SITE DESCRIPTIONS

Positions and descriptions of sites used for collecting ground-based data are useful for other analyses and remeasurement. Table C-1 lists the site numbers along with the position and site description. The starting time and the date of each collection have been included. The

position data (in degrees, minutes and seconds for latitude and longitude) were obtained from the new satellite positioning technology (the global positioning system). The error is expected to be less than 500 feet.

**Table C-1. Ground-Based Measurement Site Descriptions**

| Site No. | Time | Date (1991) | Coordinates<br>Latitude/Longitude | Description   |
|----------|------|-------------|-----------------------------------|---|
| 1        | 1330 | 7/30        | 32°21'02"<br>96°36'20"            | Wooded field, 500 ft. east of Sunridge Road   |
| 2        | 1530 | 7/30        | 32°18'31"<br>96°37'54"            | School playing field beside Ennis school building                                     |
| 3        | 945  | 7/31        | 32°19'35"<br>96°56'02"            | Meadow, southeast of the corner of Beardon Road and May Pearl Road                    |
| 4        | 1130 | 7/31        | 32°21'42"<br>96°56'33"            | In the backyard of a vacant house, northeast of Route 1496 and Hoyt Road intersection |
| 5        | 1445 | 7/31        | 32°21'29"<br>96°39'38"            | Meadow, northeast of the road intersection (Turner is one of the roads)               |
| 6        | 1630 | 7/31        | 32°20'01"<br>96°40'19"            | Meadow, south of Route 1722   |
| 7        | 1115 | 8/02        | 32°29'49"<br>96°50'50"            | Pasture, east of Route 1  |
| 8        | 1630 | 8/02        | 32°25'45"<br>96°50'26"            | Farm field, north of the Waxahachie Chamber of Commerce offices                       |
| 9        | 1130 | 8/05        | 32°13'03"<br>96°48'08"            | Farm field, south of the curve in Route 55  |
| 10       | 1420 | 8/05        | 32°24'02"<br>96°52'26"            | Fallow field, west of I-35  |
| 11       | 1600 | 8/05        | a                                 | West lawn of Ellis County courthouse, Waxahachie                                      |

<sup>a</sup> Satellite position indication was not obtained because the courthouse interfered with the satellite signals.

**Table C-1. Ground-Based Measurement Site Descriptions**

| <b>Site No.</b> | <b>Time</b> | <b>Date (1991)</b> | <b>Coordinates<br/>Latitude/Longitude</b> | <b>Description</b>   |
|-----------------|-------------|--------------------|---|--|
| 12              | 1000        | 8/06               | 32°25'23"<br>96°42'02"                    | Backyard of house, south side of Route 878                           |
| 13              | 1140        | 8/06               | 32°23'14"<br>96°48'37"                    | Vacant area east of US 287, south of Route 879                       |
| 14              | 1322        | 8/06               | 32°20'41"<br>96°49'05"                    | Park meadow, south of the north<br>Shoreline Road of Lake Waxahachie |

<sup>a</sup> Satellite position indication was not obtained because the courthouse interfered with the satellite signals.

## REFERENCES

1. Quam, W. and K. Engberg. *Low Background Ge(Li) Detector with Anticoincidence NaI Annulus*. Report No. EGG-1183-2326. EG&G/EM, Santa Barbara, California, October 1978.
2. *Low Background Ge(Li) Detector Gamma-Ray Spectroscopy System with Sample Changer*. Report No. EGG-1183-2383, S-679-R. EG&G/EM, Santa Barbara, California, October 1978.
3. *Environmental Radiation Measurements*. National Council on Radiation and Measurements. NCRP Report No. 50, Washington, D.C., December 1976, p. 30.
4. Carroll, T.R. "Airborne Soil Moisture Measurement Using Natural Terrestrial Gamma Radiation." *Soil Science*, Vol. 132, No. 5, November 1981.

## DISTRIBUTION

---

**DOE/DP**

J. E. Rudolph (3)

**DOE/NSIC**

R. S. Scott (3)

**DOE/NV**

C. A. Cox (1)

M.R. Dockter (1)

S. C. Ronshaugen (2)

**EG&G/EM**

H. W. Clark LVAO (1)

J. F. Doyle LVAO (1)

E. L. Feimster LVAO (1)

L. A. Franks SBO (1)

A. E. Fritzsch LVAO (1)

P. P. Guss WAMD (1)

T. J. Hendricks LVAO (1)

C. K. Mitchell LVAO (1)

R. A. Mohr SBO (1)

G. R. Shipman WAMD (1)

W. J. Tipton LVAO (1)

P. H. Zavattaro LVAO (1)

**DOE/HQ**

OSTI (25)

**LIBRARIES****SSCL**

RSL (30)

SBO (1)

A. Tavares (1)

TIC (1)

AN AERIAL RADIOLOGICAL SURVEY OF  
THE SUPERCONDUCTING SUPER  
COLLIDER LABORATORY  
AND SURROUNDING AREA  
WAXAHACHIE, TEXAS  
EGG-10617-1213

DATE OF SURVEY: JULY-AUGUST 1991  
DATE OF REPORT: FEBRUARY 1993

END

DATE  
FILMED

10/18/93

